Charge Retention by Gold Clusters on Surfaces Prepared Using Soft Landing of Mass Selected Ions

Grant E. Johnson,* Thomas Priest,† and Julia Laskin*

Chemical and Materials Sciences Division, Pacific Northwest National Laboratory, P.O. Box 999, MSIN K8-88, Richland, Washington 99352, United States. †Present address: Undergraduate student from Department of Bioengineering, J.B. Speed School of Engineering, University of Louisville, Louisville, Kentucky 40241, United States.

ABSTRACT Monodisperse gold clusters have been prepared on surfaces in different charge states through soft landing of mass-selected ions. Ligand-stabilized gold clusters were prepared in methanol solution by reduction of chloro(triphenylphosphine)gold(I) with borane *tert*-butylamine complex in the presence of 1,3-bis(diphenylphosphino)propane. Electrospray ionization was used to introduce the clusters into the gas phase, and mass selection was employed to isolate a single ionic cluster species ($Au_{11}L_5^{3+}$, L = 1,3-bis(diphenylphosphino)-propane), which was delivered to surfaces at well-controlled kinetic energies. Using *in situ* time-of-flight secondary ion mass spectrometry (TOF-SIMS), it is demonstrated that the $Au_{11}L_5^{3+}$ cluster retains its 3+ charge state when soft landed onto the surface of a 1*H*,1*H*,2*H*,2*H*-perfluorodecanethiol self-assembled monolayer (FSAM) on gold. In contrast, when deposited onto 16-mercaptohexadecanoic acid (COOH-SAM) and 1-dodecanethiol (HSAM) surfaces on gold, the clusters exhibit larger relative abundances of the 2+ and 1+ charge states, respectively. The kinetics of charge reduction on the FSAM and HSAM surfaces are investigated using *in situ* Fourier transform ion cyclotron resonance (FT-ICR) SIMS. It is shown that an extremely slow interfacial charge reduction occurs on the FSAM surface while an almost instantaneous neutralization takes place on the surface of the HSAM. Our results demonstrate that the size and charge state of small gold clusters on surfaces, both of which exert a dramatic influence on their chemical and physical properties, may be tuned through soft landing of mass-selected ions onto carefully selected substrates.

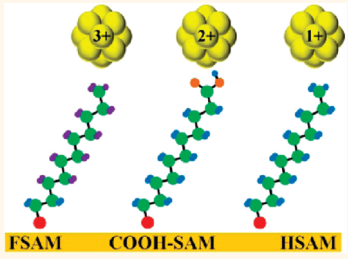

KEYWORDS: cluster · monodisperse · charge · self-assembled monolayer · electrospray ionization · soft landing

Small metal clusters are a subject of ongoing research interest due to their highly size-dependent physical and chemical properties.[1−5] The distinctive catalytic,[6,7] electronic,[8−11] and optical[12−14] characteristics of metal particles that emerge at the nanometer length scale indicate that a new generation of materials may be designed employing metal clusters either as unique functional units or as building blocks in cluster assembled materials.[15,16] Moreover, metal nanoparticles have potential for use as contrast agents in biological and cellular imaging applications, in photothermal therapeutic treatments,[17] and as composite devices for chemical sensing and threat detection.[18−20] An excellent example of the size-dependent properties of metal clusters is the reactivity of gas-phase anionic gold clusters with oxygen (O_2) and carbon monoxide (CO), which has been shown to change dramatically with the addition or removal of a single gold atom.[21] In addition, specific anionic gold clusters, Au_6^- and Au_{11}^-, have been demonstrated to exhibit greatly enhanced reactivity toward O_2 and CO, respectively, compared to anionic gold clusters of other sizes.[21,22] Analogous size-dependent behavior has been observed for subnanometer metal clusters deposited onto support materials.[23−25] For instance, the pioneering work of Heiz and Landman demonstrated that eight atom gold clusters (Au_8) supported on defect-rich magnesium oxide surfaces are the smallest clusters to promote the low-temperature oxidation of CO to carbon dioxide (CO_2).[26,27] More recently, Kaden and co-workers investigated the size-dependent activity of palladium clusters (Pd_n, $n = 1, 2, 4, 7, 10, 16, 20,$ and 25) on titanium dioxide toward the oxidation of CO to CO_2, revealing a nonmonotonic variation in catalytic activity that was strongly correlated with the Pd 3d electron binding energy of the clusters.[28] Three atom silver clusters (Ag_3) supported on alumina have been demonstrated to promote the highly selective oxidation of propylene to propylene oxide with negligible formation of the undesirable CO_2 byproduct that is normally produced with conventional catalyst materials.[29] Moreover, the high catalytic oxidation activity of gold absorbed on iron oxide has been attributed to the presence of ~0.5 nm diameter clusters containing ~10 gold atoms.[30]

* Address correspondence to grant.johnson@pnnl.gov, julia.laskin@pnnl.gov.

Received for review October 13, 2011 and accepted December 3, 2011.

Published online December 03, 2011
10.1021/nn2039565

In addition to size, the charge state of small metal clusters is known to exert a striking influence on their structure, electronic properties, and chemical reactivity. For example, ion mobility measurements of small gold clusters have shown that a transition from two-dimensional planar structures to three-dimensional geometries occurs at a cluster size of 8 atoms for cationic clusters[31] and 12 atoms for anionic clusters.[32] Furthermore, the high oxidation reactivity of gold clusters trapped at F-center defect sites has been attributed to partial electron transfer to the cluster from the underlying support material.[26] Moreover, both theoretical[33] and experimental[34] studies have demonstrated that small gold clusters on metal oxide supports can accumulate significant charge at the cluster−support interface which may serve as a unique bifunctional site for catalysis.[35] The transport of electrons through nanometer particles is known to be complex and dependent on the local chemical and physical environment.[9,36] Therefore, the nature of the charge reduction and neutralization behavior of small metal clusters is important to the function and performance of future cluster-based materials.

The fact that the size and charge state of small metal clusters have such a dramatic influence on their properties has led to a recent expansion in research efforts to chemically synthesize monodisperse clusters containing exactly a certain number of metal atoms. In general, with proper selection of capping ligands such as thiols,[37−46,52] phosphines,[42,47−51] and diphosphines[53−60] as well as careful optimization of synthesis conditions, it is possible to produce small clusters containing less than 100 atoms with relatively tight control over the final size distribution. Nevertheless, purification procedures such as fractional precipitation,[45] polyacrylamide gel electrophoresis (PAGE),[41] size exclusion chromatography,[61] or hydrodynamic fractionation[62] are typically still required to obtain truly monodisperse cluster distributions using reduction synthesis methods. An alternative approach is to synthesize clusters from a reactive metal precursor within a support material such as the pores of a zeolite which limit the cluster size.[63] The drawback to this approach is that the clusters are not accessible. Moreover, when this technique is used with high-area supports such as metal oxides, the uniformity of the cluster species is difficult to establish,[64] and even extremely well-prepared samples are not atomically monodisperse.[65] Alternative physical methods of producing metal clusters such as vapor deposition,[66] gas condensation,[67] laser vaporization,[68] magnetron sputtering combined with gas aggregation,[69] and pulsed arc synthesis[70] generate metal particles over a wide size range and, therefore, must be coupled with mass selection to isolate clusters containing a certain number of atoms.

Previous studies of gold clusters capped with bidentate diphosphine ligands such as 1,3-bis(diphenylphosphino)propane (DPPP) have shown that reduction synthesis in solution can produce multiply charged (3+, 2+) cationic clusters with an extremely narrow distribution of sizes.[53,55,57] The uniformity of the cationic clusters was established primarily through electrospray ionization[71] mass spectrometry, and the molecular formulas of the clusters were assigned based on the mass-to-charge ratios of the gas-phase ions. In the case of gold clusters capped with DPPP, the synthesis produces primarily triply charged $Au_{11}L_5^{3+}$ (L = DPPP) with smaller relative abundances of doubly charged $Au_8L_4^{2+}$, $Au_6L_4^{2+}$, and $Au_6L_3^{2+}$ clusters.[55] The large abundance of the $Au_{11}L_5^{3+}$ cluster in solution may be attributed to the high stability of the Au_{11}^{3+} core which has an electronic shell closing with 8 valence electrons.[53,72,73] Electrospray ionization, in addition to enabling the assignment of molecular formulas through mass spectrometry analysis, also produced sufficiently stable ion currents of these clusters to enable their fragmentation pathways to be studied by collision-induced dissociation, providing insight into ligand dissociation and core fission processes.[55]

These previous investigations of DPPP-capped gold clusters indicate that by combining the large ion currents obtainable by electrospray ionization with mass selection it should be possible to deposit monodisperse multiply charged gold clusters onto selected surfaces under well-controlled conditions. Indeed, in a previous publication, it was shown that soft landing of mass-selected ions may be used to prepare clean, high coverage, homogeneous samples of clusters and nanoparticles for analysis by transmission electron microscopy (TEM).[74] Moreover, the chemical functionality of the surface may be varied to investigate the charge retention and neutralization properties of the deposited cluster ions. Soft landing of polyatomic ions onto surfaces has been shown to be an effective technique for the preparation of a wide variety of materials[75−80] including model heterogeneous catalysts.[81] For example, a recent study by Nakajima and co-workers demonstrated that ion soft landing may be used to achieve facile matrix isolation of vanadium−benzene sandwich clusters.[82] In addition, previous work from our laboratory characterized the charge retention and neutralization behavior of protonated peptides, organometallic metal−salen, and ruthenium tris(bipyridine) complexes soft landed onto FSAM, HSAM, and COOH-SAM surfaces on gold.[83,84] In a related collaborative study, it was demonstrated that acid-mediated redox chemistry may be observed in thin films of organometallic complexes prepared by ion soft landing.[85] Mass selection enables species with well-defined charge and chemical composition to be delivered to surfaces. Consequently, further purification steps to remove unwanted contaminants, which are critical with solution-phase techniques, are avoided using the ion soft landing approach. This is particularly relevant for solutions of DPPP-capped gold clusters containing multiple cationic clusters, an unknown population of neutral

clusters, as well as residual reactants, solvent molecules, and negative counterions.

Herein, we demonstrate that soft landing of mass-selected ions may be used for controlled preparation of monodisperse ligand-capped gold clusters on surfaces in different charge states. To the best of our knowledge, this is the first time that charge retention by multiply charged (3+) metal clusters on surfaces has been reported. SAMs on gold, which may be terminated with a variety of different chemical functionalities, are ideal templates to test the feasibility of immobilizing monodisperse gold clusters in different charge states through soft landing and were, consequently, used as the substrates in this study.[86] Ligand-stabilized gold clusters were prepared by reduction synthesis in the presence of DPPP. Electrospray ionization was used to introduce the clusters into the gas phase, and mass selection was employed to isolate a single ionic cluster species which was delivered to the surface. Using *in situ* TOF-SIMS, it is demonstrated that the deposited $Au_{11}L_5^{3+}$ clusters retain their 3+ charge state on the FSAM surface. When soft landed onto COOH-SAM and HSAM surfaces, the clusters exhibit increased relative abundances of the 2+ and 1+ charge states, respectively. Using *in situ* FT-ICR-SIMS, the kinetics of charge reduction on the FSAM and HSAM surfaces are investigated. It is shown that an extremely slow interfacial charge reduction occurs on the FSAM surface while an almost instantaneous neutralization takes place on the surface of the HSAM. The ability to control both the size and charge state of clusters through soft landing of mass-selected ions represents a significant step forward in the nanoscale engineering of surfaces.

RESULTS AND DISCUSSION

DPPP-capped gold clusters produced by reduction synthesis in methanol/chloroform were analyzed using positive mode electrospray ionization mass spectrometry. A typical mass spectrum of a nanoparticle solution was presented in a recent publication.[74] Inspection of the mass range of m/z = 50−1500 reveals the presence of three different multiply charged cationic gold clusters: $Au_6L_3^{2+}$ at m/z = 1209.1, $Au_{11}L_5^{3+}$ at m/z = 1409.5, and $Au_6L_4^{2+}$ at m/z = 1415.7. The molecular formulas of the clusters are assigned based on their mass-to-charge ratios and the charge-state-dependent separation of the individual peaks in their isotope distributions. Moreover, the experimental spectra were compared with spectra simulated using the molecular weight calculator program (http://omics.pnl.gov/software/MWCalculator.php), and good agreement was found for each assignment. The molecular formulas also are consistent with the previous ESI-MS analyses of Bertino *et al.*,[53] who identified the $Au_{11}L_5^{3+}$ cluster, and Bergeron and Hudgens,[55] who reported $Au_6L_3^{2+}$ and $Au_{11}L_5^{3+}$. In addition to cluster species, the ESI spectrum

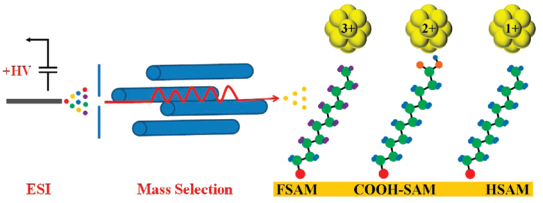

Figure 1. Schematic illustration explaining the soft landing of mass-selected gold clusters onto surfaces. The clusters are introduced into the gas phase from solution using electrospray ionization, filtered according to mass-to-charge ratio using a quadrupole mass filter, and delivered to SAM surfaces at controlled energies.

reveals the presence of molecular precursors and intermediates resulting from the reduction synthesis. In particular, AuL_2^+ m/z = 1021.3 is found to be the most abundant species within the analyzed mass range. Identical species have been observed previously for phosphine ligands $Au(PR_3)_2^+$ by Traeger *et al.*[87] and diphosphine ligands by Bergeron and Hudgens.[55] The low mass portion of the spectrum is dominated by oxidized triphenylphosphine (PPh_3O^+ m/z = 278.1), a fragment of oxidized PPh_3O^+ resulting from the loss of one phenyl group (PPh_2O^+ m/z = 201.0), oxidized DPPP (LO_2^+ m/z = 444.1), and AuL^+ m/z = 609.1. The ESI-MS spectra demonstrate that, while impressive control may be obtained over the size of cationic gold nanoclusters by proper selection of a diphosphine capping ligand[56] and synthesis conditions,[57,59] it is still extremely challenging to prepare truly monodisperse solutions of nanoparticles containing exactly a certain number of gold atoms and capping ligands. Moreover, it should be emphasized that ESI-MS only enables analysis of the ionizable components of the solution. Indeed, in a recent study, a droplet of the nanoparticle solution was cast onto a carbon-coated copper grid and analyzed by transmission electron microscopy (TEM).[74] The TEM image revealed the presence of larger 5−10 nm gold clusters that could not be observed using ESI-MS. Consequently, neutral species which may potentially account for a significant fraction of the material in solution are completely unaccounted for in the ESI-MS analysis. Electrospray ionization enables ligand-capped gold clusters to be introduced into the gas phase from solution. Employing a quadrupole mass filter, a specific cluster may then be mass-selected from the full distribution of ions and deposited in a controlled fashion onto a chosen substrate, as shown schematically in Figure 1. In this manner, a solution containing a polydisperse distribution of cationic clusters ($Au_6L_3^{2+}$, $Au_{11}L_5^{3+}$, $Au_6L_4^{2+}$) as well as an undefined population of neutral clusters may be purified to obtain atomically monodisperse clusters on a surface. Furthermore, mass selection enables molecular precursors and intermediates, negative counterions, and solvent molecules to be removed so that only the desired cluster is delivered to the surface. In this study, we mass-selected the $Au_{11}L_5^{3+}$ (m/z = 1409.5) cluster, although any cluster that

generates sufficient ion current may potentially be isolated and soft landed. The results obtained for different size gold clusters will be the subject of a forthcoming publication.

SAM surfaces were characterized *in situ* using SIMS. Typical positive mode TOF-SIMS mass spectra (m/z = 800−5000) of an FSAM surface on gold before and after soft landing of 5×10^{11} $Au_{11}L_5^{3+}$ clusters are presented in Figure 2a,b, respectively. The background spectrum obtained before deposition demonstrates that the FSAM surface is clean and contains only low mass (m/z < 1000) secondary ions characteristic of the SAM and the underlying gold substrate (data not shown).[88] Following deposition, abundances of secondary ions are observed which are consistent with the deposition of $Au_{11}L_5^{3+}$. The spectra reveal that the triply charged $Au_{11}L_5^{3+}$ (m/z = 1409.5) ion is the most abundant species on the FSAM surface, followed by the doubly charged $Au_{11}L_5^{2+}$ (m/z = 2114.2) cluster. The doubly charged species may originate from partial charge neutralization of $Au_{11}L_5^{3+}$ on the surface or from charge exchange reactions in the plume of secondary ions. No abundance was observed for the singly charged $Au_{11}L_5^{+}$ (m/z = 4228.4) cluster on the FSAM surface. In addition to the intact molecular ions, small abundances of fragment ions are observed at m/z = 1809.6 and m/z = 1021.27, which correspond to $Au_{10}L_4^{2+}$ and AuL_2^{+}, respectively. These species most likely result from fragmentation of $Au_{11}L_5^{3+}$ induced by bombardment of the surface with high-energy (15 keV) Ga^+ primary ions during TOF-SIMS analysis. The relatively low yield of these fragment ions helps to confirm that the doubly and triply charged $Au_{11}L_5^{2+/3+}$ clusters are most likely not formed through reionization during SIMS analysis but are simply desorbed from the surface. Desorption and reionization of neutralized ions is a much more destructive process which should result in large yields of fragment ions in comparison to the intact molecular ion.[89] Indeed, previous studies from our laboratory have shown that protonated Gramicidin S (GS) undergoes efficient charge neutralization when soft landed onto COOH-SAM surfaces and, consequently, exhibits large fragment yields during SIMS analysis.[90] In comparison, GS ions soft landed onto FSAM surfaces were found to retain their charge and, therefore, little fragmentation was observed during SIMS analysis.[90] To confirm the molecular assignments of the observed secondary ions, the experimental TOF-SIMS spectra were compared with the spectra simulated using the molecular weight calculator program shown as an inset in Figure 2b. Both $Au_{11}L_5^{3+}$ and $Au_{11}L_5^{2+}$ show good agreement between the measured and calculated spectra. Repeated experiments reveal that the spectra presented in Figure 2 are reproducible provided that a good quality FSAM is present on the Au surface (as confirmed by the background TOF-SIMS spectrum) and that a similar coverage of clusters is

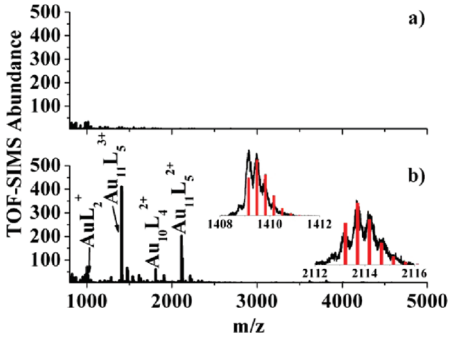

Figure 2. High-mass range of the positive mode *in situ* TOF-SIMS mass spectrum (m/z = 800−5000) of an FSAM surface before (a) and after (b) soft landing of 5×10^{11} $Au_{11}L_5^{3+}$ (L = DPPP) (m/z = 1409.5) clusters.

delivered to the surface in each experiment (5×10^{11} clusters in this particular study).

The results presented in Figure 2b demonstrate that it is possible to prepare atomically monodisperse gold clusters on surfaces through soft landing of mass-selected ions and that the 3+ charge state of the ion may be partially preserved on the FSAM surface. This is particularly relevant in the case of $Au_{11}L_5^{3+}$ because this triply charged species is a noble gas "superatomic" cluster with a closed electronic shell containing 8 valence electrons.[53,72,73] The charge retention properties of the FSAM surface observed in the current experiments are consistent with previous results[75] which demonstrated that protonated peptides[89,91−95] and organometallic ions[83,85] soft landed onto FSAM surfaces also retain their charge. In particular, multiply protonated peptides have been observed to retain both one and two protons on the FSAM surface,[89,93] and the charge reduction and desorption kinetics of the peptides have been measured and fitted to a kinetic model.[92] Furthermore, singly charged organometallic ions (Co(III)(salen)$^+$, Mn(III)(salen)$^+$ and V(V)O-(salen)$^+$, salen = *N*,*N*′-ethylenebis(salicylideneaminato) ligand) were also observed to retain the majority of their charge when soft landed onto FSAM surfaces.[83] In the case of the V(V)O(salen)$^+$ complex, the charge retention properties of the FSAM surface were sufficient to enable reduction−oxidation reactivity to be observed on the surface between the deposited organometallic ions and proton donor molecules.[85] The slow electron transport properties through fluorinated SAMs have been characterized using a variety of techniques and are generally attributed to interface dipoles which create a charge barrier to electron transport at the CF_3/vacuum interface.[96−98] Our experiments indicate that the charge barrier is high enough that the triply charged gold cluster ions retain their charge for days if left in vacuum and even if exposed to atmospheric conditions. Surprisingly, a surface that was sonicated in ethanol and subjected to subsequent analysis by TOF-SIMS still exhibited measurable abundances of the 3+ and 2+ ions. This

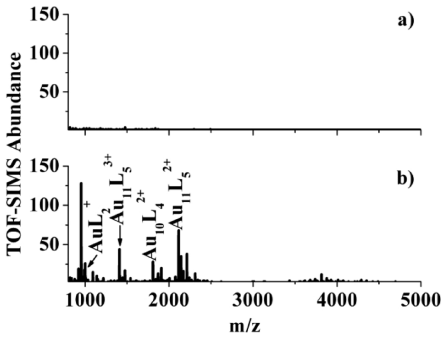

Figure 3. High-mass range of the positive mode *in situ* TOF-SIMS mass spectrum (m/z = 800−5000) of a COOH-SAM surface before (a) and after (b) soft landing of 5×10^{11} $Au_{11}L_5^{3+}$ (L = DPPP) (m/z = 1409.5) clusters.

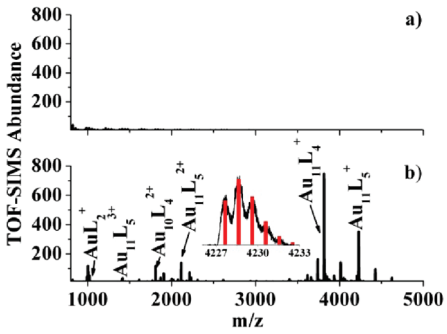

Figure 4. High-mass range of the positive mode *in situ* TOF-SIMS mass spectrum (m/z = 800−5000) of an HSAM surface before (a) and after (b) soft landing of 5×10^{11} $Au_{11}L_5^{3+}$ (L = DPPP) (m/z = 1409.5) clusters.

indicates that the FSAM efficiently retains the charge of the cluster and that the ion-induced dipole interaction (mirror potential) of the cluster with the underlying gold substrate serves to immobilize the cluster on the surface so that it is not washed away during sonication in solution. Moreover, the results suggest that the 2+ ions observed on the FSAM surface result from charge neutralization that occurs at the time of collision with the surface.

The TOF-SIMS spectra obtained before and after soft landing of 5×10^{11} $Au_{11}L_5^{3+}$ clusters onto a COOH-SAM surface on gold are presented in Figure 3a,b, respectively. Similar to the results for the FSAM surface, the spectrum obtained prior to deposition shows that the COOH-SAM surface is clean and contains only peaks characteristic of the monolayer and underlying gold surface. The spectrum obtained following soft landing exhibits the same peaks as in the FSAM spectrum, albeit with very different relative abundances. In the case of the COOH-SAM surface, the most abundant molecular ion corresponds to the doubly charged $Au_{11}L_5^{2+}$ (m/z = 2114.2) cluster. The triply charged $Au_{11}L_5^{3+}$ (m/z = 1409.5) cluster is relatively less abundant, and a very small yield of the singly charged $Au_{11}L_5^{+}$ (m/z = 4228.4) cluster is also observed. This is in sharp contrast to the results obtained on the FSAM surface where the triply charged $Au_{11}L_5^{3+}$ was by far the most abundant species and the singly charged $Au_{11}L_5^{+}$ cluster was not observed at all. Larger relative abundances of fragment ions, including AuL_2^{+} and $Au_{10}L_4^{2+}$, were also observed on the COOH-SAM in comparison to the FSAM surface. The charge retention observed in the current study is consistent with earlier findings for small doubly charged organometallic ions such as ruthenium tris(bipyridine) $Ru(bpy)_3^{2+}$ which retained a portion of their charge when soft landed onto COOH-SAM surfaces.[84] The current results, however, are in contrast with the observations for protonated peptides deposited onto COOH-SAM surfaces which were found to be efficiently neutralized.[89,93] Based on the fact that the $Au_{11}L_5^{3+}$ clusters are native ions and not molecules that are ionized through protonation like peptides, it is reasonable that their behavior is similar to other native ions such as $Ru(bpy)_3^{2+}$. In the case of molecules that are ionized through protonation, charge neutralization following SL occurs through loss of the proton to the surface. In comparison, native ions such as $Au_{11}L_5^{3+}$ and $Ru(bpy)_3^{2+}$ are neutralized by a different mechanism involving electron transfer through the SAM from the underlying substrate. As mentioned in the previous paragraph, SAMs are capable of withstanding significant potentials before electron tunneling through the monolayer takes place. It should also be mentioned that soft landing of cationic clusters onto the COOH-terminated SAM likely results in a stronger surface immobilization than deposition onto the FSAM surface. This is due to the strong electrostatic interaction between the negative carboxylate anions (COO^-) on the surface and the positively charged cluster. In a previous study, we demonstrated that soft landing of doubly charged $Ru(bpy)_3^{2+}$ ions onto COOH-SAMs results in the formation of a strongly bound adduct which serves to anchor the organometallic complex to the surface.[84] A similar strategy has also been employed to attach the same $Ru(bpy)_3^{2+}$ complex to silica-coated silver nanoparticles in the solution phase through a linker molecule containing two carboxylate groups.[99] The electrostatic interaction between the $Ru(bpy)_3^{2+}$ cation and the carboxylate anions was strong enough that the hybrid material was able to promote catalytic photooxidation reactions.

The charge retention and neutralization of $Au_{11}L_5^{3+}$ clusters soft landed onto an HSAM surface are demonstrated in the TOF-SIMS spectrum presented in Figure 4b. A reference spectrum of the HSAM obtained before cluster deposition, shown in Figure 4a, demonstrates that the surface is clean and contains a self-assembled monolayer. The spectrum taken after soft landing on the HSAM reveals a situation that is very different to that following deposition on the FSAM and COOH-SAM surfaces. In particular, the most abundant intact molecular ion is now the singly charged $Au_{11}L_5^{+}$ cluster (m/z = 4228.4). The inset in Figure 4b shows a comparison between the experimental and calculated spectra for $Au_{11}L_5^{+}$, which exhibits very good agreement, providing

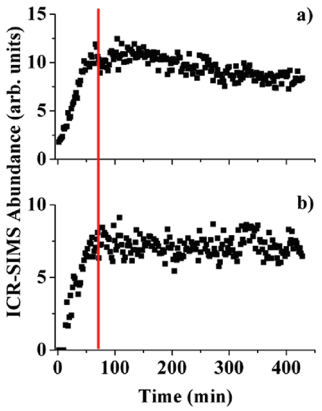

Figure 5. *In situ* FT-ICR-SIMS abundance of (a) $Au_{11}L_5^{3+}$ (m/z = 1409.5) and (b) $Au_{11}L_5^{2+}$ (m/z = 2114.2) during and after soft landing of 10^{11} $Au_{11}L_5^{3+}$ onto an FSAM surface. The red line indicates the end of soft landing.

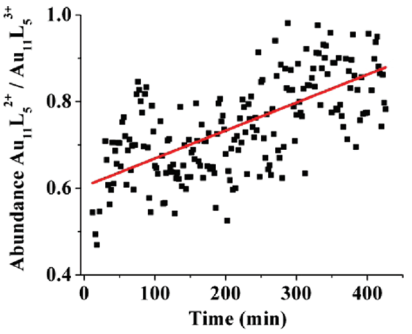

Figure 6. *In situ* FT-ICR-SIMS abundance ratio of $Au_{11}L_5^{2+}$ (m/z = 2114.2) to $Au_{11}L_5^{3+}$ (m/z = 1409.5) during and after soft landing of $Au_{11}L_5^{3+}$ onto an FSAM surface. The red line is a linear fit to the experimental data.

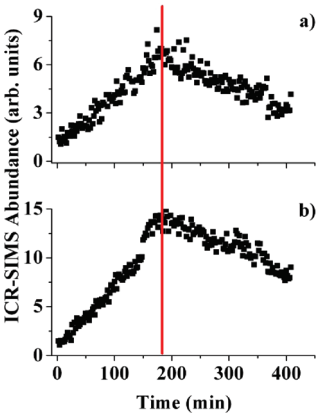

Figure 7. *In situ* FT-ICR-SIMS abundance of (a) $Au_{11}L_5^{+}$ (m/z = 4228.4) and (b) $Au_{11}L_4^{+}$ (m/z = 3816.2) during and after soft landing of $10^{11}Au_{11}L_5^{3+}$ onto an HSAM surface. The red line indicates the end of soft landing.

further support for the peak assignment. A significant abundance of the doubly charged $Au_{11}L_5^{2+}$ cluster (m/z = 2114.2) is also observed, and the triply charged cluster $Au_{11}L_5^{3+}$ (m/z = 1409.5) is found to be the least abundant molecular ion. Moreover, the $Au_{11}L_4^{+}$ fragment ion that results from the loss of one diphosphine ligand from $Au_{11}L_5^{+}$ is shown to be the most abundant ion in the spectrum. The lower charge state of the gold cluster and the large fragment yield obtained on the HSAM surface suggest that some of the clusters are neutralized rapidly upon deposition and that both desorption and reionization are necessary to detect deposited material by TOF-SIMS. The rapid charge reduction of gold clusters deposited onto the HSAM surface is consistent with previous finding from our laboratory, which demonstrated that organometallic ions[83] are efficiently neutralized when soft landed onto HSAMs. Multiply protonated peptide ions, in contrast, were found to partially retain one proton on the HSAM surface[93] and to lose all protons on the COOH-SAM. The results presented for gold clusters, therefore, are very similar to previous findings for organometallic metal–salen complexes.

To gain more insight into the charge retention and neutralization kinetics of cationic gold clusters soft landed onto different SAMs, we conducted an *in situ* FT-ICR-SIMS experiment, which enables the analysis of surface composition both during and after ion deposition. In this fashion, the abundance of different cluster charge states on the surface may be monitored over a period of several hours. The results for $Au_{11}L_5^{3+}$ deposited onto the FSAM surface are shown in Figure 5. During deposition, both the triply charged $Au_{11}L_5^{3+}$ and doubly charged $Au_{11}L_5^{2+}$ clusters exhibit a linear increase in abundance with the triply charged ion being the more abundant species. Following the end of soft landing, the triply charged cluster exhibits a slow decrease in relative abundance over a period of 5 h, as shown in Figure 5a. In contrast, Figure 5b indicates that the doubly charged cluster exhibits a steady abundance that does not change appreciably over this period of time. The ratio of the abundance of $Au_{11}L_5^{2+}$ to $Au_{11}L_5^{3+}$ exhibits a clear increase over time, as shown in Figure 6. This behavior is consistent with a mechanism where slow transfer of electrons through the FSAM monolayer results in charge reduction of $Au_{11}L_5^{3+}$ producing $Au_{11}L_5^{2+}$.

$$Au_{11}L_5^{3+} + e \rightarrow Au_{11}L_5^{2+} \quad (1)$$

These FT-ICR-SIMS results confirm the findings of the TOF-SIMS analysis presented in Figure 2b, which also showed the triply charged cluster to be the most abundant molecular ion, both immediately following deposition, after the surface had been stored for several days in vacuum, and following ultrasonic washing in ethanol.

Soft landing on the FSAM surface results in the most charge retention of the deposited ions, while clusters deposited on the HSAM surface appear to undergo rapid charge neutralization. Therefore, we also employed the FT-ICR-SIMS technique to better characterize the charge neutralization kinetics of $Au_{11}L_5^{3+}$ clusters soft landed onto the HSAM surface. The results, presented in Figure 7, demonstrate that the triply charged clusters are indeed

rapidly neutralized upon collision with the surface. In fact, no doubly or triply charged ions could be detected during the FT-ICR-SIMS analysis, which is in contrast to the TOF-SIMS results where low abundances of both $Au_{11}L_5^{3+}$ and $Au_{11}L_5^{2+}$ were detected on the HSAM surface. This is likely due to the lower sensitivity of the FT-ICR-SIMS technique in comparison to TOF-SIMS.[100] During the FT-ICR-SIMS analysis, the most abundant ions were found to be $Au_{11}L_5^{+}$ and the fragment ion, $Au_{11}L_4^{+}$. Both of these species exhibit a linear growth in abundance during soft landing and a rapid decrease in abundance following the end of deposition. These results provide further evidence that the triply charged $Au_{11}L_5^{3+}$ ions are neutralized almost instantaneously upon deposition. Moreover, because the clusters are neutralized, they no longer have an ion-induced dipole (mirror potential) interaction with the underlying gold substrate to hold them in place. It is probable, therefore, that the rapid decrease in the abundance of the singly charged clusters following the end of deposition results from desorption from the surface at the room temperature conditions at which the experiments are conducted. It is also possible that localized heating from bombardment of the surface with the 8 kV Cs^+ primary ions serves to accelerate the desorption process.

CONCLUSIONS

The results presented herein demonstrate that monodisperse gold clusters may be prepared on surfaces in different charge states using soft landing of mass-selected ions onto carefully chosen substrates. Specifically, ligand-capped gold clusters may be produced through solution-phase reduction synthesis, introduced into the gas phase using electrospray ionization, isolated according to mass-to-charge ratio, and deposited onto surfaces under well-controlled conditions. Evidence obtained by *in situ* TOF and FT-ICR-SIMS indicates that by changing the terminal functionality of self-assembled monolayer surfaces on gold from FSAM, to COOH-SAM, to HSAM, it is possible to tune the most abundant charge state of deposited $Au_{11}L_5$ clusters from 3+, to 2+, to 1+, respectively. Moreover, spectra acquired over extended periods of time show that the charged clusters are stable in vacuum and, in the case of the FSAM surface, in ambient conditions and even in solvent environments. The results demonstrate that the size and charge state of small metal clusters, both of which are known to significantly influence their chemical and physical properties, may be controlled on surfaces through soft landing onto appropriate substrates.

METHODS

Nanoparticle Synthesis. Ligand-capped gold clusters were synthesized in solution according to literature procedures.[53−58] Briefly, a gold precursor, chloro(triphenylphosphine)gold(I) (99.9% Sigma-Aldrich), was dissolved in a 1/1 mixture of methanol and chloroform (Sigma-Aldrich) to create 100 mL of a 0.1 mM solution. A bidentate capping ligand, 1,3-bis(diphenylphosphino)propane (97% Sigma-Aldrich), was then added to a concentration 0.1 mM. After mixing of the gold precursor and capping ligand, a weak reducing agent, borane *tert*-butylamine (97% Sigma-Aldrich), was added to a final solution concentration of 0.5 mM. The solution was stirred rapidly at room temperature for 3 h until it turned a deep orange color indicating the reduction of Au(I) and the formation of gold nanoparticles. The nanoparticle solutions were stored in the dark at room temperature in Pyrex jars. The nanoparticle solutions were diluted for use in electrospray ionization without any further purification.

Formation of Self-Assembled Monolayer Surfaces on Gold. The gold substrates used to create alkyl thiol self-assembled monolayers were purchased from Platypus Technologies (Madison, WI) and have the following specifications: 10 × 10 mm, 525 μm thick Si, 50 Å Ti adhesion layer, 1000 Å Au layer. 1*H*,1*H*,2*H*,2*H*-Perfluorodecanethiol (FSAM), 16-mercaptohexadecanoic acid (COOH-SAM), and 1-dodecanethiol (HSAM) were purchased from Sigma-Aldrich. The FSAM, COOH-SAM, and HSAM surfaces were prepared following literature procedures[101,102] using nondenatured ethanol as the solvent, which was also purchased from Sigma-Aldrich. The acetic acid used for the preparation of the COOH-SAM surfaces was purchased from Fisher Scientific. The gold substrates were ultrasonically washed in ethanol, cleaned using a Boekel (Boekel Scientific, Feasterville, PA) ultraviolet cleaner, and immersed in glass scintillation vials containing 1 mM solutions of thiol in an ethanol solvent for the FSAM and HSAM and a 2% acetic acid solution in ethanol for the COOH-SAM. The monolayers were allowed to assemble for at least 12 h and then ultrasonically washed for 5 min in ethanol. The surfaces were then rinsed with pure ethanol, dried with nitrogen (N_2), and mounted in the SIMS sample holder.

ESI-MS Analysis of Nanoparticle Solution. Electrospray ionization[103] mass spectra (ESI-MS) (m/z = 50−1500) of the gold nanoparticle solutions were obtained in the positive ion mode using a Bruker HCT ion trap mass spectrometer (Bruker Daltonics, Bremen, Germany). A spray potential of 4 kV was employed, and the potential gradient in the source region of the instrument was kept at <5 V to minimize in-source fragmentation. The nanoparticle solutions were diluted by a factor of 10 in pure methanol and introduced at a flow rate of 0.05 mL/h using a syringe pump.

Soft Landing of Mass Selected Ions. The soft landing experiments were conducted employing a custom-built instrument coupled to a time-of-flight secondary ion mass spectrometer (TOF-SIMS) which has been described in detail elsewhere.[100] Briefly, triply charged $Au_{11}L_5^{3+}$ ions were generated through electrospray ionization,[103] introduced into vacuum using an electrodynamic ion funnel,[104] focused in a collision quadrupole, mass-selected with a quadrupole mass filter, deflected 90° by a quadrupole bender, and transferred to the surface through a series of two einzel lenses. An optimized ion current of ∼40 pA was directed at the surface for 2 h, corresponding to a total delivery of 5×10^{11} ions to a circular spot approximately 3 mm in diameter. The kinetic energy of the ions impacting the surface was controlled by adjusting the potentials applied to the second collision quadrupole and the surface and was set at ∼20 eV for all of the experiments described herein. Assuming that all of the ions retain their charge once deposited onto the surface, the maximum potential resulting from the total charge delivered by the ion beam to the surface can be estimated[94] and was calculated to be ∼0.4 V for 5×10^{11} triply charged $Au_{11}L_5^{3+}$ ions delivered to a spot size of 3 mm. Because this potential is much smaller than the kinetic energy of the ions, it does not interfere with ion deposition. It follows that all of the ions delivered to the substrate are able to approach the surface and can become immobilized.

***In Situ* TOF-SIMS Analysis.** *In situ* analysis of surfaces was performed using 15 keV Ga^+ TOF-SIMS in a commercial PHI TRIFT II instrument (Physical Electronics, Eden Prairie, MN). In TOF-SIMS, the sample is bombarded by 15 keV primary gallium ions (Ga^+, 500 pA, 5 ns pulse width, 10 kHz repetition rate) which induces desorption of material from the surface. The positive secondary ions ejected from the surface are extracted into the mass analyzer which consists of three separate electrostatic sectors. The mass spectrometer compensates for the kinetic energy dispersion of the secondary ions and achieves a mass resolution of around 4000 at 1000 amu. All positive mode spectra were acquired at the center of the deposited spot for 2 min. Negative mode spectra were not obtained.

***In Situ* FT-ICR-SIMS Analysis.** Experiments were performed using a specially designed 6T FT-ICR instrument configured for studying ion−surface interactions.[88,92,105] Briefly, mass-selected cluster ions produced in a high-transmission electrospray source undergo normal-incidence collision with a SAM surface positioned at the rear trapping plate of the ICR cell. During ion SL, the surface is exposed to a continuous beam of mass selected ions. *In situ* analysis of surfaces during and following SL is performed by combining 8 keV Cs^+ secondary ion mass spectrometry with FT-ICR detection of the sputtered positive ions (FT-ICR-SIMS).[92] Static SIMS conditions with a total ion flux of about 10^{10} ions/cm^2 (current 4 nA, duration 80 μs, spot diameter 4.6 mm, 10 shots per spectrum, ~200 data points) were used in these experiments that typically lasted for 6 h. Each SIMS spectrum was averaged over 10 shots corresponding to an acquisition time of 10 s. The kinetics data were obtained by sampling the SAM surface every 2 min for approximately 6 h.

Acknowledgment. The authors acknowledge support for this research by a grant from the U.S. Department of Energy (DOE), Office of Basic Energy Sciences, Division of Chemical Sciences, Geosciences, and Biosciences and the Laboratory Directed Research and Development Program at the Pacific Northwest National Laboratory (PNNL). This work was performed at the W.R. Wiley Environmental Molecular Sciences Laboratory (EMSL), a national scientific user facility sponsored by the U.S. DOE of Biological and Environmental Research and located at PNNL. PNNL is operated by Battelle for the U.S. DOE. T.P. acknowledges support from the DOE Science Undergraduate Laboratory Internship (SULI) program at Pacific Northwest National Laboratory (PNNL). G.E.J. is grateful for the support of the Linus Pauling Distinguished Postdoctoral Fellowship Program at PNNL.

REFERENCES AND NOTES

1. Castleman, A. W.; Jena, P. Clusters: A Bridge between Disciplines. *Proc. Natl. Acad. Sci. U.S.A.* **2006**, *103*, 10552–10553.
2. Castleman, A. W.; Jena, P. Clusters: A Bridge across the Disciplines of Environment, Materials Science, and Biology. *Proc. Natl. Acad. Sci. U.S.A.* **2006**, *103*, 10554–10559.
3. Jena, P.; Castleman, A. W. Clusters: A Bridge across the Disciplines of Physics and Chemistry. *Proc. Natl. Acad. Sci. U.S.A.* **2006**, *103*, 10560–10569.
4. Knight, W. D.; Clemenger, K.; Deheer, W. A.; Saunders, W. A.; Chou, M. Y.; Cohen, M. L. Electronic Shell Structure and Abundances of Sodium Clusters. *Phys. Rev. Lett.* **1984**, *52*, 2141–2143.
5. Brack, M. The Physics of Simple Metal-Clusters: Self-Consistent Jellium Model and Semiclassical Approaches. *Rev. Mod. Phys* **1993**, *65*, 677–732.
6. Haruta, M. Size- and Support-Dependency in the Catalysis of Gold. *Catal. Today* **1997**, *36*, 153–166.
7. Heiz, U.; Abbet, S.; Sanchez, A.; Schneider, W. D.; Hakkinen, H.; Landman, U. Chemical Reactions on Size-Selected Clusters on Surfaces. *Nobel Symp.* **2001**, *117*, 87–98.
8. Nichols, R. J.; Gittins, D. I.; Bethell, D.; Schiffrin, D. J. A Nanometre-Scale Electronic Switch Consisting of a Metal Cluster and Redox-Addressable Groups. *Nature* **2000**, *408*, 67–69.
9. Weiss, P. S.; Smith, R. K.; Nanayakkara, S. U.; Woehrle, G. H.; Pearl, T. P.; Blake, M. M.; Hutchison, J. E. Spectral Diffusion in the Tunneling Spectra of Ligand-Stabilized Undecagold Clusters. *J. Am. Chem. Soc.* **2006**, *128*, 9266–9267.
10. Ahmadi, T. S.; Logunov, S. L.; El Sayed, M. A. Size-Dependent Electron Dynamics of Gold Nanoparticles. *Acs. Sym. Ser.* **1997**, *679*, 125–140.
11. Logunov, S. L.; Ahmadi, T. S.; El Sayed, M. A.; Khoury, J. T.; Whetten, R. L. Electron Dynamics of Passivated Gold Nanocrystals Probed by Subpicosecond Transient Absorption Spectroscopy. *J. Phys. Chem. B* **1997**, *101*, 3713–3719.
12. Murray, R. W.; Parker, J. F.; Fields-Zinna, C. A. The Story of a Monodisperse Gold Nanoparticle: $Au_{25}L_{18}$. *Acc. Chem. Res.* **2010**, *43*, 1289–1296.
13. El-Sayed, M. A.; Link, S. Size and Temperature Dependence of the Plasmon Absorption of Colloidal Gold Nanoparticles. *J. Phys. Chem. B* **1999**, *103*, 4212–4217.
14. Sun, Y. G.; Gray, S. K.; Peng, S. Surface Chemistry: A Non-negligible Parameter in Determining Optical Properties of Small Colloidal Metal Nanoparticles. *Phys. Chem. Chem. Phys.* **2011**, *13*, 11814–11826.
15. Castleman, A. W.; Claridge, S. A.; Khanna, S. N.; Murray, C. B.; Sen, A.; Weiss, P. S. Cluster-Assembled Materials. *ACS Nano* **2009**, *3*, 244–255.
16. Castleman, A. W.; Khanna, S. N. Clusters, Superatoms, and Building Blocks of New Materials. *J. Phys. Chem. C* **2009**, *113*, 2664–2675.
17. El-Sayed, M. A.; Jain, P. K.; Lee, K. S.; El-Sayed, I. H. Calculated Absorption and Scattering Properties of Gold Nanoparticles of Different Size, Shape, and Composition: Applications in Biological Imaging and Biomedicine. *J. Phys. Chem. B* **2006**, *110*, 7238–7248.
18. Willner, I.; Balogh, D.; Tel-Vered, R.; Freeman, R. Photochemically and Electrochemically Triggered Au Nanoparticles "Sponges". *J. Am. Chem. Soc.* **2011**, *133*, 6533–6536.
19. Tian, H.; Zhang, J. J.; Riskin, M.; Freeman, R.; Tel-Vered, R.; Balogh, D.; Willner, I. Electrochemically Triggered Au Nanoparticles "Sponges" for the Controlled Uptake and Release of a Photoisomerizable Dithienylethene Guest Substrate. *ACS Nano* **2011**, *5*, 5936–5944.
20. Willner, I.; Riskin, M.; Ben-Amram, Y.; Tel-Vered, R.; Chegel, V.; Almog, J. Molecularly Imprinted Au Nanoparticles Composites on Au Surfaces for the Surface Plasmon Resonance Detection of Pentaerythritol Tetranitrate, Nitroglycerin, and Ethylene Glycol Dinitrate. *Anal. Chem.* **2011**, *83*, 3082–3088.
21. Bernhardt, T. M. Gas-Phase Kinetics and Catalytic Reactions of Small Silver and Gold Clusters. *Int. J. Mass. Spectrom.* **2005**, *243*, 1–29.
22. Kim, Y. D. Chemical Properties of Mass-Selected Coinage Metal Cluster Anions: Towards Obtaining Molecular-Level Understanding of Nanocatalysis. *Int. J. Mass. Spectrom.* **2004**, *238*, 17–31.
23. Abbet, S.; Judai, K.; Klinger, L.; Heiz, U. Synthesis of Monodispersed Model Catalysts Using Softlanding Cluster Deposition. *Pure Appl. Chem.* **2002**, *74*, 1527–1535.
24. Abbet, S.; Sanchez, A.; Heiz, U.; Schneider, W. D.; Ferrari, A. M.; Pacchioni, G.; Rosch, N. Size-Effects in the Acetylene Cyclotrimerization on Supported Size-Selected Pd_N Clusters ($1 \leq N \leq 30$). *Surf. Sci.* **2000**, *454*, 984–989.
25. Landman, U.; Yoon, B.; Zhang, C.; Heiz, U.; Arenz, M. Factors in Gold Nanocatalysis: Oxidation of CO in the Non-scalable Size Regime. *Top. Catal.* **2007**, *44*, 145–158.
26. Yoon, B.; Hakkinen, H.; Landman, U.; Worz, A. S.; Antonietti, J. M.; Abbet, S.; Judai, K.; Heiz, U. Charging Effects on Bonding and Catalyzed Oxidation of CO on Au_8 Clusters on MgO. *Science* **2005**, *307*, 403–407.
27. Sanchez, A.; Abbet, S.; Heiz, U.; Schneider, W. D.; Hakkinen, H.; Barnett, R. N.; Landman, U. When Gold Is Not Noble: Nanoscale Gold Catalysts. *J. Phys. Chem. A* **1999**, *103*, 9573–9578.
28. Anderson, S. L.; Kaden, W. E.; Wu, T. P.; Kunkel, W. A. Electronic Structure Controls Reactivity of Size-Selected Pd Clusters Adsorbed on TiO_2 Surfaces. *Science* **2009**, *326*, 826–829.

29. Curtiss, L. A.; Lei, Y.; Mehmood, F.; Lee, S.; Greeley, J.; Lee, B.; Seifert, S.; Winans, R. E.; Elam, J. W.; Meyer, R. J.; *et al.* Increased Silver Activity for Direct Propylene Epoxidation *via* Subnanometer Size Effects. *Science* **2010**, *328*, 224–228.
30. Kiely, C. J.; Herzing, A. A.; Carley, A. F.; Landon, P.; Hutchings, G. J. Identification of Active Gold Nanoclusters on Iron Oxide Supports for CO Oxidation. *Science* **2008**, *321*, 1331–1335.
31. Gilb, S.; Weis, P.; Furche, F.; Ahlrichs, R.; Kappes, M. M. Structures of Small Gold Cluster Cations (Au_N^+, $N < 14$): Ion Mobility Measurements *versus* Density Functional Calculations. *J. Chem. Phys.* **2002**, *116*, 4094–4101.
32. Furche, F.; Ahlrichs, R.; Weis, P.; Jacob, C.; Gilb, S.; Bierweiler, T.; Kappes, M. M. The Structures of Small Gold Cluster Anions As Determined by a Combination of Ion Mobility Measurements and Density Functional Calculations. *J. Chem. Phys.* **2002**, *117*, 6982–6990.
33. Yoon, B.; Landman, U. Electric Field Control of Structure, Dimensionality, and Reactivity of Gold Nanoclusters on Metal-Supported MgO Films. *Phys. Rev. Lett.* **2008**, *100*, 056102.
34. Nilius, N.; Lin, X.; Freund, H. J.; Walter, M.; Frondelius, P.; Honkala, K.; Hakkinen, H. Quantum Well States in Two-Dimensional Gold Clusters on MgO Thin Films. *Phys. Rev. Lett.* **2009**, *102*, 206801.
35. Molina, L. M.; Hammer, B. Active Role of Oxide Support during CO Oxidation at Au/MgO. *Phys. Rev. Lett.* **2003**, *90*, 206102.
36. Parsons, G. N.; Chu, C. W.; Na, J. S. Conductivity in Alkylamine/Gold and Alkanethiol/Gold Molecular Junctions Measured in Molecule/Nanoparticle/Molecule Bridges and Conducting Probe Structures. *J. Am. Chem. Soc.* **2007**, *129*, 2287–2296.
37. Jin, R. C.; Zhu, Y.; Qian, H. F. Quantum-Sized Gold Nanoclusters: Bridging the Gap between Organometallics and Nanocrystals. *Chem.—Eur. J.* **2011**, *17*, 6584–6593.
38. Jin, R. C. Quantum Sized, Thiolate-Protected Gold Nanoclusters. *Nanoscale* **2010**, *2*, 343–362.
39. Jin, R. C.; Wu, Z. K.; Lanni, E.; Chen, W. Q.; Bier, M. E.; Ly, D. High Yield, Large Scale Synthesis of Thiolate-Protected Ag_7 Clusters. *J. Am. Chem. Soc.* **2009**, *131*, 16672–16674.
40. Dass, A.; Nimmala, P. R. $Au_{36}SPh_{23}$ Nanomolecules. *J. Am. Chem. Soc.* **2011**, *133*, 9175–9177.
41. Tsukuda, T.; Shichibu, Y.; Negishi, Y.; Tsunoyama, H.; Kanehara, M.; Teranishi, T. Extremely High Stability of Glutathionate-Protected Au_{25} Clusters against Core Etching. *Small* **2007**, *3*, 835–839.
42. Tsukuda, T.; Shichibu, Y.; Negishi, Y.; Teranishi, T. Large-Scale Synthesis of Thiolated Au_{25} Clusters *via* Ligand Exchange Reactions of Phosphine-Stabilized Au_{11} Clusters. *J. Am. Chem. Soc.* **2005**, *127*, 13464–13465.
43. Tsukuda, T.; Negishi, Y.; Takasugi, Y.; Sato, S.; Yao, H.; Kimura, K. Magic-Numbered Au_N Clusters Protected by Glutathione Monolayers (N = 18, 21, 25, 28, 32, 39): Isolation and Spectroscopic Characterization. *J. Am. Chem. Soc.* **2004**, *126*, 6518–6519.
44. Tsukuda, T.; Negishi, Y.; Nobusada, K. Glutathione-Protected Gold Clusters Revisited: Bridging the Gap between Gold(I)−Thiolate Complexes and Thiolate-Protected Gold Nanocrystals. *J. Am. Chem. Soc.* **2005**, *127*, 5261–5270.
45. Kornberg, R. D.; Levi-Kalisman, Y.; Jadzinsky, P. D.; Kalisman, N.; Tsunoyama, H.; Tsukuda, T.; Bushnell, D. A. Synthesis and Characterization of Au_{102}(P-Mba)$_{44}$ Nanoparticles. *J. Am. Chem. Soc.* **2011**, *133*, 2976–2982.
46. Tracy, J. B.; Crowe, M. C.; Parker, J. F.; Hampe, O.; Fields-Zinna, C. A.; Dass, A.; Murray, R. W. Electrospray Ionization Mass Spectrometry of Uniform and Mixed Monolayer Nanoparticles: $Au_{25}[S(CH_2)_2Ph]_{18}$ and $Au_{25}[S(CH_2)_2Ph]_{18-x}SR_x$. *J. Am. Chem. Soc.* **2007**, *129*, 16209–16215.
47. Malatest., L; Naldini, L.; Simonett., G; Cariati, F. Triphenylphosphine−Gold(0)Gold(I) Compounds. *Chem. Commun.* **1965**, 212–213.
48. Mingos, D. M. P. Gold—A Flexible Friend in Cluster Chemistry. *J. Chem. Soc., Dalton Trans.* **1996**, 561–566.
49. Mingos, D. M. P. Structure and Bonding in Cluster Compounds of Gold. *Polyhedron* **1984**, *3*, 1289–1297.
50. Li, J.; Zhang, H. F.; Stender, M.; Zhang, R.; Wang, C. M.; Wang, L. S. Toward the Solution Synthesis of the Tetrahedral Au_{20} Cluster. *J. Phys. Chem. B* **2004**, *108*, 12259–12263.
51. Evans, D. G.; Mingos, D. M. P. Molecular-Orbital Analysis of the Bonding in Penta-nuclear and Hepta-nuclear Gold Tertiary Phosphine Clusters. *J. Organomet. Chem.* **1985**, *295*, 389–400.
52. Hamouda, R.; Bellina, B.; Bertorelle, F.; Compagnon, I.; Antoine, R.; Broyer, M.; Rayane, D.; Dugourd, P. Electron Emission of Gas-Phase $[Au_{25}SG_{18}\text{-}6H]^{7-}$ Gold Cluster and Its Action Spectroscopy. *J. Phys. Chem. Lett.* **2010**, *1*, 3189–3194.
53. Bertino, M. F.; Sun, Z. M.; Zhang, R.; Wang, L. S. Facile Syntheses of Monodisperse Ultrasmall Au Clusters. *J. Phys. Chem. B* **2006**, *110*, 21416–21418.
54. Bergeron, D. E.; Coskuner, O.; Hudgens, J. W.; Gonzalez, C. A. Ligand Exchange Reactions in the Formation of Diphosphine-Protected Gold Clusters. *J. Phys. Chem. C* **2008**, *112*, 12808–12814.
55. Bergeron, D. E.; Hudgens, J. W. Ligand Dissociation and Core Fission from Diphosphine-Protected Gold Clusters. *J. Phys. Chem. C* **2007**, *111*, 8195–8201.
56. Castleman, A. W.; Golightly, J. S.; Gao, L.; Bergeron, D. E.; Hudgens, J. W.; Magyar, R. J.; Gonzalez, C. A. Impact of Swapping Ethyl for Phenyl Groups on Diphosphine-Protected Undecagold. *J. Phys. Chem. C* **2007**, *111*, 14625–14627.
57. Hudgens, J. W.; Pettibone, J. M. Synthetic Approach for Tunable, Size-Selective Formation of Monodisperse, Diphosphine-Protected Gold Nanoclusters. *J. Phys. Chem. Lett.* **2010**, *1*, 2536–2540.
58. Hudgens, J. W.; Pettibone, J. M. Gold Cluster Formation with Phosphine Ligands: Etching as a Size-Selective Synthetic Pathway for Small Clusters? *ACS Nano* **2011**, *5*, 2989–3002.
59. Konishi, K.; Shichibu, Y. HCl-Induced Nuclearity Convergence in Diphosphine-Protected Ultrasmall Gold Clusters: A Novel Synthetic Route to "Magic-Number" Au_{13} Clusters. *Small* **2010**, *6*, 1216–1220.
60. Orlov, A.; Zhao, S.; Ramakrishnan, G.; Su, D.; Rieger, R.; Koller, A. Novel Photocatalytic Applications of Sub-nanometer Gold Particles for Environmental Liquid and Gas Phase Reactions. *Appl. Catal. B* **2011**, *104*, 239–244.
61. Dass, A.; Knoppe, S.; Boudon, J.; Dolamic, I.; Burgi, T. Size Exclusion Chromatography for Semipreparative Scale Separation of $Au_{38}SR_{24}$ and $Au_{40}SR_{24}$ and Larger Clusters. *Anal. Chem.* **2011**, *83*, 5056–5061.
62. Hackley, V. A.; Tsai, D. H.; Cho, T. J.; DelRio, F. W.; Taurozzi, J.; Zachariah, M. R. Hydrodynamic Fractionation of Finite Size Gold Nanoparticle Clusters. *J. Am. Chem. Soc.* **2011**, *133*, 8884–8887.
63. Gates, B. C.; Fierro-Gonzalez, J. C.; Hao, Y. L. Gold Nanoclusters Entrapped in the Alpha-Cages of Y Zeolites: Structural Characterization by X-ray Absorption Spectroscopy. *J. Phys. Chem. C* **2007**, *111*, 6645–6651.
64. Guzman, J.; Gates, B. C. Gold Nanoclusters Supported on MgO: Synthesis, Characterization, and Evidence of Au_6. *Nano Lett.* **2001**, *1*, 689–692.
65. Gates, B. C.; Uzun, A.; Ortalan, V.; Hao, Y. L.; Browning, N. D. Nanoclusters of Gold on a High-Area Support: Almost Uniform Nanoclusters Imaged by Scanning Transmission Electron Microscopy. *ACS Nano* **2009**, *3*, 3691–3695.
66. Goodman, D. W.; Lai, X. F. Structure−Reactivity Correlations for Oxide-Supported Metal Catalysts: New Perspectives from STM. *J. Mol. Catal. A* **2000**, *162*, 33–50.
67. Goldby, I. M.; vonIssendorff, B.; Kuipers, L.; Palmer, R. E. Gas Condensation Source for Production and Deposition of Size-Selected Metal Clusters. *Rev. Sci. Instrum.* **1997**, *68*, 3327–3334.
68. Wagner, R. L.; Vann, W. D.; Castleman, A. W. A Technique for Efficiently Generating Bimetallic Clusters. *Rev. Sci. Instrum.* **1997**, *68*, 3010–3013.
69. Pratontep, S.; Carroll, S. J.; Xirouchaki, C.; Streun, M.; Palmer, R. E. Size-Selected Cluster Beam Source Based

on Radio Frequency Magnetron Plasma Sputtering and Gas Condensation. *Rev. Sci. Instrum.* **2005**, *76*, 045103.
70. Klipp, B.; Grass, M.; Muller, J.; Stolcic, D.; Lutz, U.; Gantefor, G.; Schlenker, T.; Boneberg, J.; Leiderer, P. Deposition of Mass-Selected Cluster Ions Using a Pulsed Arc Cluster-Ion Source. *Appl. Phys. A* **2001**, *73*, 547–554.
71. Fenn, J. B.; Mann, M.; Meng, C. K.; Wong, S. F.; Whitehouse, C. M. Electrospray Ionization-Principles and Practice. *Mass Spectrom. Rev.* **1990**, *9*, 37–70.
72. Mingos, D. M. P. Molecular-Orbital Calculations on Cluster Compounds of Gold. *J. Chem. Soc., Dalton Trans.* **1976**, 1163–1169.
73. Walter, M.; Akola, J.; Lopez-Acevedo, O.; Jadzinsky, P. D.; Calero, G.; Ackerson, C. J.; Whetten, R. L.; Gronbeck, H.; Hakkinen, H. A Unified View of Ligand-Protected Gold Clusters as Superatom Complexes. *Proc. Natl. Acad. Sci. U.S.A.* **2008**, *105*, 9157–9162.
74. Johnson, G. E.; Wang, C.; Priest, T.; Laskin, J. Monodisperse Au_{11} Clusters Prepared by Soft Landing of Mass Selected Ions. *Anal. Chem.* **2011**, *83*, 8069–8072.
75. Miller, S. A.; Luo, H.; Pachuta, S. J.; Cooks, R. G. Soft-Landing of Polyatomic Ions at Fluorinated Self-Assembled Monolayer Surfaces. *Science* **1997**, *275*, 1447–1450.
76. Ouyang, Z.; Takats, Z.; Blake, T. A.; Gologan, B.; Guymon, A. J.; Wiseman, J. M.; Oliver, J. C.; Davisson, V. J.; Cooks, R. G. Preparing Protein Microarrays by Soft-Landing of Mass-Selected Ions. *Science* **2003**, *301*, 1351–1354.
77. Cooks, R. G.; Gologan, B.; Green, J. R.; Alvarez, J.; Laskin, J. Ion/Surface Reactions and Ion Soft-Landing. *Phys. Chem. Chem. Phys.* **2005**, *7*, 1490–1500.
78. Davila, S. J.; Birdwell, D. O.; Verbeck, G. F. Drift Tube Soft-Landing for the Production and Characterization of Materials: Applied to Cu Clusters. *Rev. Sci. Instrum.* **2010**, *81*, 034104.
79. Cooks, R. G.; Badu-Tawiah, A. K.; Wu, C. P. Ambient Ion Soft Landing. *Anal. Chem.* **2011**, *83*, 2648–2654.
80. Cooks, R. G.; Cyriac, J.; Li, G. T. Vibrational Spectroscopy and Mass Spectrometry for Characterization of Soft Landed Polyatomic Molecules. *Anal. Chem.* **2011**, *83*, 5114–5121.
81. Heiz, U.; Bullock, E. L. Fundamental Aspects of Catalysis on Supported Metal Clusters. *J. Mater. Chem.* **2004**, *14*, 564–577.
82. Nakajima, A.; Nagaoka, S.; Matsumoto, T.; Okada, E.; Mitsui, M. Room-Temperature Isolation of $V(Benzene)_2$ Sandwich Clusters *via* Soft-Landing into *N*-Alkanethiol Self-Assembled Monolayers. *J. Phys. Chem. B* **2006**, *110*, 16008–16017.
83. Laskin, J.; Wang, P.; Hadjar, O. Soft-Landing of Co(III)-$Salen^+$ and Mn(III)$Salen^+$ on Self-Assembled Monolayer Surfaces. *J. Phys. Chem. C* **2010**, *114*, 5305–5311.
84. Laskin, J.; Johnson, G. E. Preparation of Surface Organometallic Catalysts by Gas-Phase Ligand Stripping and Reactive Landing of Mass-Selected Ions. *Chem.—Eur. J.* **2010**, *16*, 14433–14438.
85. Cooks, R. G.; Peng, W. P.; Johnson, G. E.; Fortmeyer, I. C.; Wang, P.; Hadjar, O.; Laskin, J. Redox Chemistry in Thin Layers of Organometallic Complexes Prepared Using Ion Soft Landing. *Phys. Chem. Chem. Phys.* **2011**, *13*, 267–275.
86. Love, J. C.; Estroff, L. A.; Kriebel, J. K.; Nuzzo, R. G.; Whitesides, G. M. Self-Assembled Monolayers of Thiolates on Metals as a Form of Nanotechnology. *Chem. Rev.* **2005**, *105*, 1103–1169.
87. Colton, R.; Harrison, K. L.; Mah, Y. A.; Traeger, J. C. Cationic Phosphine Complexes of Gold(I)—An Electrospray Mass-Spectrometric Study. *Inorg. Chim. Acta* **1995**, *231*, 65–71.
88. Alvarez, J.; Cooks, R. G.; Barlow, S. E.; Gaspar, D. J.; Futrell, J. H.; Laskin, J. Preparation and *In Situ* Characterization of Surfaces Using Soft Landing in a Fourier Transform Ion Cyclotron Resonance Mass Spectrometer. *Anal. Chem.* **2005**, *77*, 3452–3460.
89. Laskin, J.; Wang, P.; Hadjar, O.; Futrell, J. H.; Alvarez, J.; Cooks, Z. G. Charge Retention by Peptide Ions Soft-Landed onto Self-Assembled Monolayer Surfaces. *Int. J. Mass Spectrom.* **2007**, *265*, 237–243.
90. Hadjar, O.; Wang, P.; Futrell, J. H.; Laskin, J. Effect of the Surface on Charge Reduction and Desorption Kinetics of Soft Landed Peptide Ions. *J. Am. Soc. Mass Spectrom.* **2009**, *20*, 901–906.
91. Alvarez, J.; Futrell, J. H.; Laskin, J. Soft-Landing of Peptides onto Self-Assembled Monolayer Surfaces. *J. Phys. Chem. A* **2006**, *110*, 1678–1687.
92. Laskin, J.; Hadjar, O.; Futrell, J. H. First Observation of Charge Reduction and Desorption Kinetics of Multiply Protonated Peptides Soft Landed onto Self-Assembled Monolayer Surfaces. *J. Phys. Chem. C* **2007**, *111*, 18220–18225.
93. Laskin, J.; Hadjar, O.; Wang, P.; Futrell, J. H. Effect of the Surface on Charge Reduction and Desorption Kinetics of Soft Landed Peptide Ions. *J. Am. Soc. Mass Spectrom.* **2009**, *20*, 901–906.
94. Laskin, J.; Wang, P.; Hadjar, O. Soft-Landing of Peptide Ions onto Self-Assembled Monolayer Surfaces: An Overview. *Phys. Chem. Chem. Phys.* **2008**, *10*, 1079–1090.
95. Johnson, G. E.; Hu, Q.; Laskin, J. Soft Landing of Complex Molecules on Surfaces. *Annu. Rev. Anal. Chem.* **2011**, *4*, 83–104.
96. Alloway, D. M.; Hofmann, M.; Smith, D. L.; Gruhn, N. E.; Graham, A. L.; Colorado, R.; Wysocki, V. H.; Lee, T. R.; Lee, P. A.; Armstrong, N. R. Interface Dipoles Arising from Self-Assembled Monolayers on Gold: UV-Photoemission Studies of Alkanethiols and Partially Fluorinated Alkanethiols. *J. Phys. Chem. B* **2003**, *107*, 11690–11699.
97. Armstrong, N. R.; Alloway, D. M.; Graham, A. L.; Yang, X.; Mudalige, A.; Colorado, R.; Wysocki, V. H.; Pemberton, J. E.; Lee, T. R.; Wysocki, R. J. Tuning the Effective Work Function of Gold and Silver Using Omega-Functionalized Alkanethiols: Varying Surface Composition through Dilution and Choice of Terminal Groups. *J. Phys. Chem. C* **2009**, *113*, 20328–20334.
98. Pflaum, J.; Bracco, G.; Schreiber, F.; Colorado, R.; Shmakova, O. E.; Lee, T. R.; Scoles, G.; Kahn, A. Structure and Electronic Properties of Ch3- and Cf3-Terminated Alkanethiol Monolayers on Au(111): A Scanning Tunneling Microscopy, Surface X-ray and Helium Scattering Study. *Surf. Sci.* **2002**, *498*, 89–104.
99. Mori, K.; Kawashima, M.; Che, M.; Yamashita, H. Enhancement of the Photoinduced Oxidation Activity of a Ruthenium(II) Complex Anchored on Silica-Coated Silver Nanoparticles by Localized Surface Plasmon Resonance. *Angew. Chem., Int. Ed* **2010**, *49*, 8598–8601.
100. Johnson, G. E.; Lysonski, M.; Laskin, J. *In Situ* Reactivity and TOF-SIMS Analysis of Surfaces Prepared by Soft and Reactive Landing of Mass-Selected Ions. *Anal. Chem.* **2010**, *82*, 5718–5727.
101. Chidsey, C. E. D.; Liu, G. Y.; Rowntree, P.; Scoles, G. Molecular Order at the Surface of an Organic Monolayer Studied by Low-Energy Helium Diffraction. *J. Chem. Phys.* **1989**, *91*, 4421–4423.
102. Wang, H.; Chen, S. F.; Li, L. Y.; Jiang, S. Y. Improved Method for the Preparation of Carboxylic Acid and Amine Terminated Self-Assembled Monolayers of Alkanethiolates. *Langmuir* **2005**, *21*, 2633–2636.
103. Fenn, J. B.; Mann, M.; Meng, C. K.; Wong, S. F.; Whitehouse, C. M. Electrospray Ionization for Mass-Spectrometry of Large Biomolecules. *Science* **1989**, *246*, 64–71.
104. Kelly, R. T.; Tolmachev, A. V.; Page, J. S.; Tang, K. Q.; Smith, R. D. The Ion Funnel: Theory, Implementations, and Applications. *Mass Spectrom. Rev.* **2010**, *29*, 294–312.
105. Laskin, J.; Denisov, E. V.; Shukla, A. K.; Barlow, S. E.; Futrell, J. H. Surface-Induced Dissociation in a Fourier Transform Ion Cyclotron Resonance Mass Spectrometer: Instrument Design and Evaluation. *Anal. Chem.* **2002**, *74*, 3255–3261.